[6] Johnson, W. A. and McRuer, D. T., "A System Model for Low-Level Approach," AIAA Paper 70-1034, Santa Barbara, Calif., 1970.

[7] Weir, D. H., Klein, R. H., and McRuer, D. T., "Principles for the Design of Advanced Flight Director Systems Based on the Theory of Manual Control Displays," CR-1748, March 1971, NASA.

[8] McRuer, D. T. and Jex, H. R., "A Review of Quasi-Linear Pilot Models," *IEEE Transactions*, Vol. HFE-8, No. 3, Sept. 1967, pp. 231–249.

[9] McRuer, D., Graham, D., Krendel, E., and Reisener, W., Jr., "Human Pilot Dynamics in Compensatory Systems—Theory, Models, and Experiments with Controlled Element and Forcing Function Variations," AFFDL-TR-65-15, July 1965, Air Force Flight Dynamics Lab., Wright-Patterson Air Force Base, Ohio.

[10] McRuer, D. and Weir, D. H., "Theory of Manual Vehicular Control," *Ergonomics*, Vol. 12, No. 4, 1969, pp. 599–663.

NOVEMBER 1971 J. AIRCRAFT VOL. 8, NO. 11

Measurement and Analysis of Pilot Scanning Behavior during Simulated Instrument Approaches

DAVID H. WEIR* AND RICHARD H. KLEIN†
Systems Technology, Inc., Hawthorne, Calif.

Experimental measurements of pilot scanning and control response in a simulated instrument approach are reported. Airline pilot subjects flew ILS approaches in a six degree-of-freedom fixed base DC-8 simulator at the NASA Ames Research Center. A conventional instrument panel and controls were used, with simulated vertical gust and glide slope beam bend forcing functions. Pilot eye fixations and scan traffic on the panel were measured using a recently developed eye point-of-regard (EPR) system. Simultaneous recordings were made of displayed signals, pilot response, and vehicle motions. The EPR data were reduced for 31 approaches with a cross section of subjects to obtain dwell times, look rates, scan rates, and fractional scanning workload. Flight director (zero reader) approaches as well as standard localizer/glide slope (manual) approaches were made. The scanning results showed the attitude and glide slope/localizer instruments to be primary in a manual ILS approach, sharing 70–80% of the pilot's attention. The glide slope/localizer instrument required shorter dwell times with a fixed instrument sensitivity. Differences in dwell time between pilots occurred mainly on the attitude instrument. With the flight director, glide path deviation errors were reduced and the flight director instrument dominated pilot attention (about 80%). There were no apparent circulatory scanning patterns in any of the approaches. These EPR results were generally consistent with prior data where meaningful comparisons could be made.

Introduction

FURTHER development and validation of the theory of manual control displays[1,2] required measurement and analysis of simultaneous eye movement and pilot response data in flight control tasks under realistic instrument conditions. The objective of the research program reported herein was to obtain such data for instrument approach tasks, and to reduce the eye point-of-regard (EPR) data to the scanning statistics needed to continue development of the theory. Data are now in hand for several airline pilots in more than a hundred simulated instrument approaches in a subsonic jet transport. The scanning statistics for a cross section of 31 two-minute runs are described and analyzed in this paper. They are part of the data base for ongoing efforts to correlate EPR with pilot response and displayed motion variables.

Presented as Paper 70-999 at the AIAA Guidance, Control and Flight Mechanics Conference, Santa Barbara, Calif., Aug. 17–19, 1970; submitted Sept. 11, 1970; revision received April 29, 1971. This paper includes research efforts supported by the NASA Ames Research Center, Moffett Field, Calif., under Contract NAS2-3746.

Index categories: Aircraft Handling, Stability, and Control; Research Facilities and Instrumentation.

* Principal Research Engineer. Member AIAA.

† Senior Research Engineer. Member AIAA.

Background

Early research in this area measured the instrument scanning patterns of pilots in a variety of actual IFR maneuvers,[4–8] but no records were made of the instrument readings or pilot responses. Stable statistical traffic patterns appeared in their results for various pilots and maneuvers. More recent research (Refs. 9–11) has been concerned mainly with statistical models of the scanning process, rather than with the establishment of connections with the causal factors of the displayed signals. Again, the displayed signals were either not recorded or not correlated against the scanning behavior, or the definition of the controlled element dynamics was incomplete.

These past studies have used eye movement cameras, electro-oculographics, or corneal reflection techniques; which tend to be expensive, difficult to operate, and detrimental to the experimental environment. An eye point-of-regard system recently developed by STI (Systems Technology Inc.) avoids many of these problems. It measures the horizontal and vertical movement of the eye with respect to the head by a corneal-schleral boundary contrast technique and the head movement relative to the panel reference by electromechanical means. These signals are combined in a special purpose computer to obtain overall eye point-of-regard. Figure 1 shows the device in use. This, plus proven

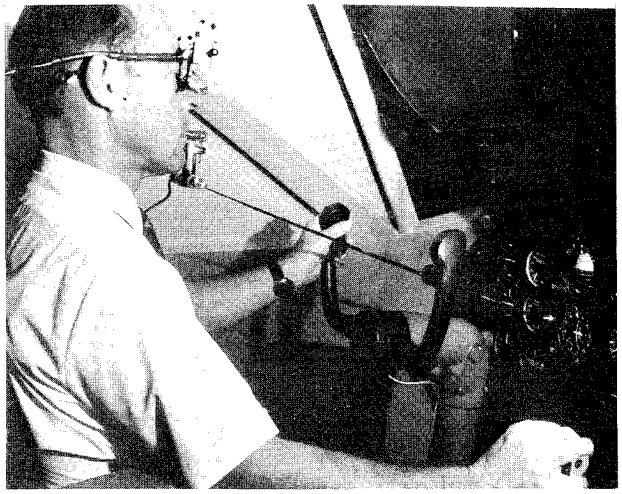

Fig. 1 EPR system in use.

experimental techniques for measuring pilot dynamic response in multiloop tasks,[12,13] and the availability of a high fidelity simulation facility at the NASA Ames Research Center, gave the tools to accomplish the behavioral measurement program.

Experimental Situations

This study used a NASA Ames fixed-base six degree-of-freedom simulator, configured as a DC-8 transport in the landing approach configuration. The task was to fly an instrument landing system (ILS) approach from the outer marker (30,000 ft from threshold) to the middle marker (2500 ft from threshold) in the presence of vertical gusts and glide slope beam bends. Aircraft motions, displayed signals, pilot response, and eye point-of-regard were recorded. The system block diagram is shown in Fig. 2. Details of the experimental setup, vehicle transfer functions, and procedures used are given in Ref. 3.

The main experimental configurations are described in Table 1. Configurations *B*, *C*, and *D* displayed localizer and glide slope deviation, pitch and roll attitude, and peripheral instruments; but no director display. These tasks varied in their detail in order to explore effects of scanning and statistical stationarity. Configurations *E* and *F* employed all the displays of *C* and *D*, respectively, plus a standard lateral and longitudinal director display superimposed on the artificial horizon instrument. Other tasks included a pitch-attitude only tracking task designed to provide single loop response data on the present subjects for correlation with past data and models, and visual breakout runs involving transition from the panel display to the external visual field, inside the middle marker.

The panel configuration was the standard "T," typical of current transport usage. The layout for the manual ILS configurations is shown in Fig. 3, where the instrument needles have been deleted for clarity. For all configurations, Instrument 2 contained a conventional attitude ball displaying pitch and roll attitude relative to a fiducial horizon line. The two-axis director bar also appeared on Instrument 2 for Configurations *E* and *F*. Vertical and horizontal crosspointers on Instrument 5 displayed localizer and glide slope deviations, respectively.

Two independent longitudinal forcing functions were used, a pitch attitude command (θ_c) and a glide slope deviation command (G_c). The pitch attitude forcing function simulated a random appearing 5 ft/sec rms vertical gust input with a bandwidth of 0.8 rad/sec and an equivalent rms amplitude of 1.2°, as shown in Fig. 4. The glide slope command forcing function simulated low-frequency beam bends with an effective bandwidth of about 0.3 rad/sec. It had an rms amplitude of 0.04° path angle, or about 0.2 dots of needle deflection, as shown in Fig. 5. This permits multiloop describing functions to be computed from the data. Tracers, consisting of one or two low-amplitude sine waves, were added to some other displayed signals.

Each pilot was told to try to keep the glide slope and localizer needles centered at all times. As a result, the approaches were all within acceptable limits at the minimum descent altitude. A data recording session usually involved five or six 100 sec runs in succession, divided at random between manual ILS and flight director configurations. Fixed range and varying range configurations were not mixed in the same session, but were run on separate days.

Pilot Subjects

Seven participated in the program, and data for three of them have been analyzed. The subjects were all current professional airline jet pilots or copilots, and reflected a cross section of age and background. Pilot 1 was a senior instructor captain with multiengine piston and jet bomber experience. Pilot 2, a younger copilot, transitioned into commercial flying from general aviation/light aircraft. Pilot 3, a young copilot, had extensive prior military single-engine fighter/bomber experience. The simulation was sufficiently similar to their current experience that the pilots were able to achieve a stable level of proficiency within a few runs.

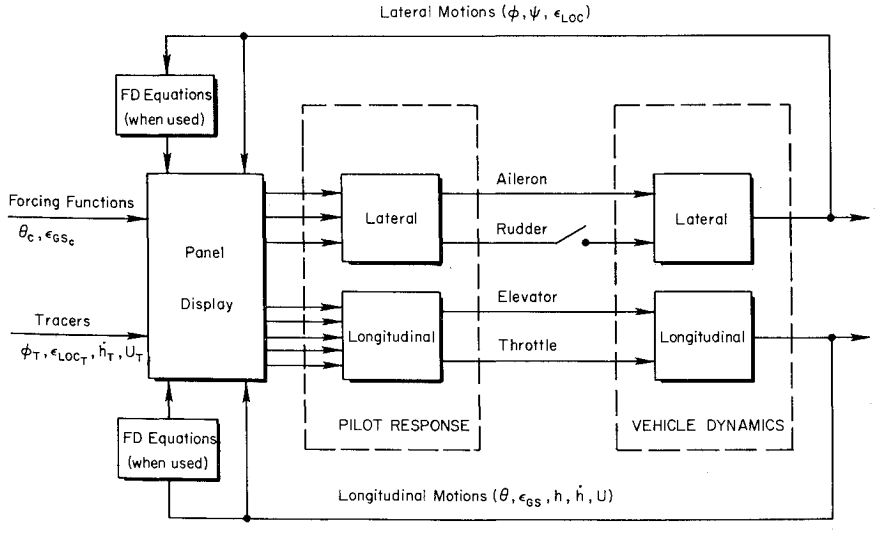

Fig. 2 Block diagram of experimental task.

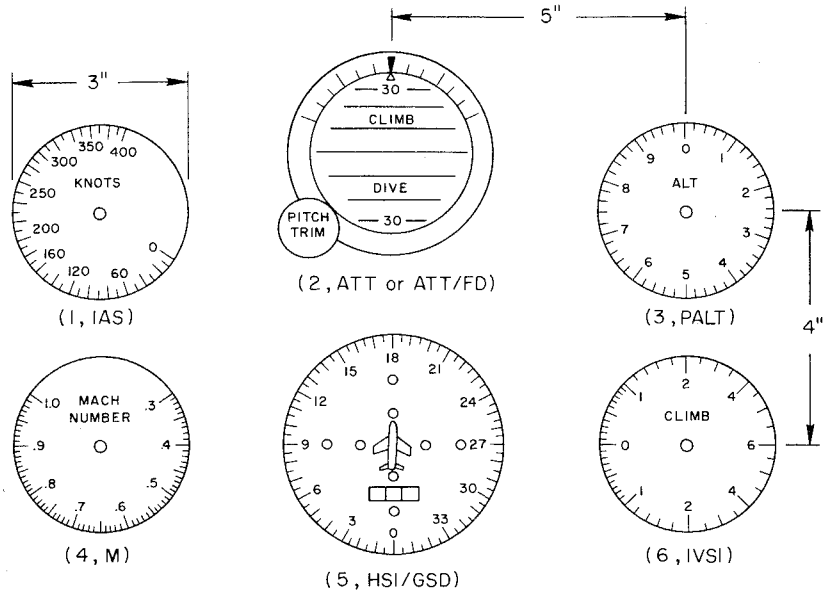

Fig. 3 Layout of basic flight instruments.

Scanning Traffic Definitions

Some definitions of the properties of the raw and reduced EPR data are needed. For a given run of T_R sec duration: M is the number of instruments, N_i is the number of fixations on Instrument i, N_M is the total number of fixations on all instruments, and N is the total number of fixations on instruments, elsewhere, blinks, etc. It follows that

$$N_M = \sum_{i=1}^{M} N_i$$

The duration of a look at a given instrument is called the "dwell time," T_d, and

$T_{d_{i_k}}$ is the duration of the kth dwell on Instrument i

$$T_i = \sum_{k=1}^{N_i} T_{d_{i_k}} \text{ is the total time fixating } i$$

$$T_R = \sum_{i=1}^{M} T_i + T_{\text{other}}$$

Table 1 Experimental configurations

Configuration	Description	Purpose	Instructions to subjects
B (Split-axis manual ILS, fixed-range)	Three degree-of-freedom longitudinal task. Forcing functions and tracers on. Lateral axes under autopilot control, but meters visible. No director.	Provide longitudinal scanning task, and basis for validating multiloop pilot response model.	Simulates a split-axis manual approach under Category II conditions. Control only the longitudinal motions. An autopilot is controlling the lateral motions. There is some turbulence. Try to keep the glide slope needle centered at all times.
C (Manual ILS, fixed-range)	All-axis approach task with forcing functions and tracers on. The glide slope deviation computer range was fixed at 30,000 ft from threshold. The altimeter and rate-of-climb meters appeared normal (varying range). No director.	Provides stationary all-axis task. Reference case for comparison with split-axis, range-varying, and director cases.	Simulates a Category II manual ILS approach. There is some turbulence. Try to keep the glide slope and localizer needles centered at all times.
D (Manual ILS, varying-range)	All-axis approach task with forcing functions and tracers on. The range varied throughout the run. Glide slope deviation per unit altitude error increases with decreasing range. No director.	Provides nonstationary longitudinal task. Typical of "old fashioned" cross pointer ILS display.	
E (Director, fixed-range)	All-axis approach task with forcing functions and tracers on. Director on, and driven by forcing function. Same as configuration *C* plus flight director.	Provides equalized, integrated display and stationary all-axis task. Reference director case. Typical of modern practice.	Simulates a Category II director approach. There is some turbulence. Use the director to follow the approach path, keeping the glide slope and localizer needles centered. Pitch commands must be obeyed immediately to avoid a standoff. The glide slope and localizer needles must be monitored.
F (Director, varying-range)	All-axis approach task with forcing functions and tracers. Director on. Glide slope component of FD forcing function attenuated with range by director computer. Same as *E*, except range-varying.	Provides equalized, integrated display but non-stationary forcing function.	

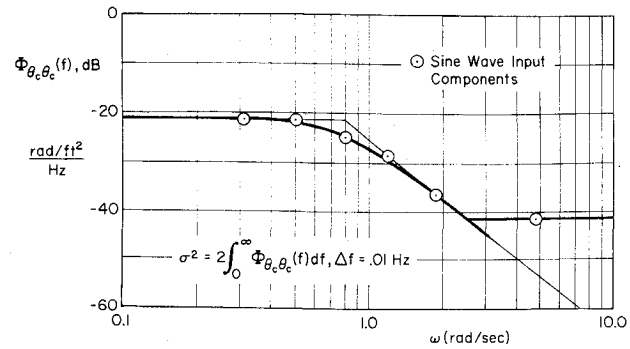

Fig. 4 Power spectral density of pitch angle forcing function.

where T_{other} includes blinks and looks elsewhere than at the defined instruments. For data reduction convenience we assign a number to blinks and other regions of the panel so that all time during the run is subscripted and allocated.

Average properties of the data are important. The mean dwell time on Instrument i is

$$\bar{T}_{d_i} = \frac{1}{N_i}\sum_{k=1}^{N_i} T_{d_{i_k}} = \frac{T_i}{N_i}$$

The scan rate over all instruments on the panel is the average number of fixations per second, given by

$$\bar{f}_s = N/T_R$$

The scan rate on a given instrument is called the look rate, given by

$$\bar{f}_{s_i} = N_i/T_R$$

The fraction of fixations on the ith instrument, ν_i, is called the look fraction,

$$\nu_i = N_i/N$$

The dwell fraction is the fraction of time spent on Instrument i, given by

$$\eta_i = T_i/T_R$$

This is also called the fractional scanning workload. The look interval is the inverse of the scanning workload,

$$\bar{T}_{s_i} = 1/\bar{f}_{s_i}$$

The look interval is a measure of the recycle time, and it can also be computed from the individual scan intervals (the time between successive looks at an instrument).

Data Reduction Procedure

The six instruments, shown in Fig. 3, and other regions of the panel were numbered for analysis as shown in Fig. 6. Looks at region 8 were usually blinks, and they resulted in

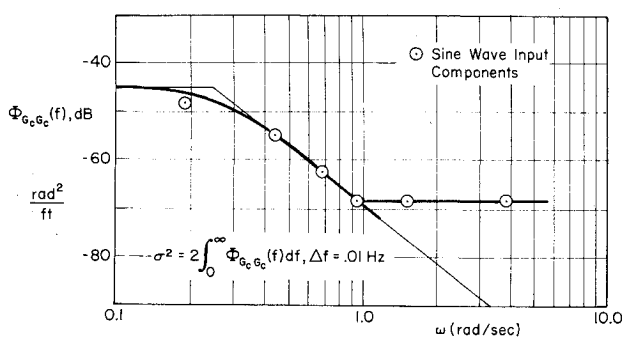

Fig. 5 Power spectral density of glide slope forcing function.

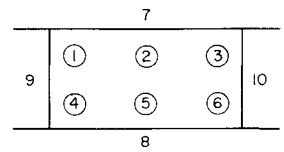

Fig. 6 EPR regions on instrument panel.

the total workload on the instruments being less than unity. There were essentially no looks at regions 7, 9, and 10.

The eye point-of-regard is defined by vertical and horizontal coordinates on the panel. A typical segment of data is shown in Fig. 7. The major part of the dwell is well defined. The transitions are defined as having a duration no greater than 0.15 sec. Typical vertical transition times (over all pilots) between instruments are in the range 0.06–0.09 sec. The horizontal transitions are slightly faster, 0.05–0.08 sec. The difference probably reflects eyelid lag on the vertical channel, which varies between subjects. If the transition times are longer than 0.15 sec they become an actual look, blink, etc. The transition times are allocated to the adjacent dwells in roughly equal proportions as shown in Fig. 7. A Fortran IV program was used to compute the dwell time statistics defined above, histograms for each instrument, summations for all instruments, and one way link transitions between instruments.

Scanning Statistics

A cross section of 31 runs representing three subjects was selected for detailed analysis. The selected runs are listed in Table 2. Each cell is denoted by a shorthand notation, e.g., $C1$ is configuration C with Pilot 1. Pilot 1 was the principal subject and replications for each configuration are shown. Runs for Pilots 2 and 3 help define interpilot and interconfiguration differences.

The detailed scanning statistics for each of the 31 runs were averaged over a given pilot/configuration cell to obtain Table 3. The look rates, $\bar{f}_{s_i}$, and dwell times, $\bar{T}_{d_i}$, in Table 3 were examined to determine similarities and differences among the pilots and configurations. The results of these statistical tests and other observations are discussed below.

Stationarity within a Run

A key question in computing average scanning statistics during landing approach is whether there is any significant change in the pilot's scanning behavior as the approach progresses. One potential source of nonstationarity arises in the glide slope deviation bar and pitch director whose gains change in the range varying configurations. Several of the range varying runs were processed in three successive intervals as shown in Table 4. The mean dwell time and dwell fraction for each of the five instruments for three typical 100 sec runs were compared in order to determine if the scanning statistics were nonstationary. In general, the mean dwell times do not

Table 2 Summary of runs analyzed

Configuration	Subject 1	Subject 2	Subject 3
B (Split-axis manual ILS, fixed-range)	*B*1 — Two runs	*B*2 — One run	
C (Manual ILS, fixed-range)	*C*1 — Five runs	*C*2 — Five runs	
D (Manual ILS, varying-range)	*D*1 — Five runs		
E (FD, fixed-range)	*E*1 — Four runs	*E*2 — Three runs	
F (FD, varying-range)	*F*1 — Three runs		*F*3 — One run

Table 3 Average scanning statistics

Conf.	Subj.	No. runs avg.	Instrument 1, IAS						Instrument 2, ATT or ATT/FD					
			N_1	$\bar{T}_{d1}$	σ_{T1}	$\bar{f}_{s1}$	η_1	ν_1	N_2	$\bar{T}_{d2}$	σ_{T2}	$\bar{f}_{s2}$	η_2	ν_2
B	1	2	18	0.57	0.18	0.09	0.051	0.068	89	0.67	0.29	0.446	0.296	0.337
B	2	1	2	0.64	0.05	0.02	0.013	0.015	61	0.82	0.36	0.607	0.498	0.462
C	1	5	25	0.69	0.28	0.05	0.034	0.042	238	0.74	0.33	0.474	0.353	0.397
C	2	5	1	0.63	0	0.002	0.001	0.002	254	0.95	0.33	0.511	0.483	0.453
D	1	5	43	0.69	0.35	0.085	0.059	0.066	282	0.81	0.38	0.560	0.452	0.431
D	3	2	3	0.88	0.40	0.015	0.013	0.013	85	1.00	0.45	0.423	0.425	0.357
E	1	4	44	0.55	0.15	0.110	0.06	0.113	171	1.73	1.72	0.428	0.739	0.438
E	2	3	13	0.54	0.11	0.043	0.023	0.070	84	3.03	3.41	0.276	0.836	0.454
F	1	3	53	0.56	0.15	0.177	0.099	0.163	147	1.50	1.36	0.492	0.737	0.453
F	3	1	6	0.59	0.10	0.059	0.035	0.079	37	2.19	1.80	0.366	0.80	0.487

Conf.	Subj.	No. runs avg.	Instrument 3, PALT						Instrument 5, HSI/GSD					
			N_3	$\bar{T}_{d3}$	σ_{T3}	$\bar{f}_{s3}$	η_3	ν_3	N_5	$\bar{T}_{d5}$	σ_{T5}	$\bar{f}_{s5}$	η_5	ν_5
B	1	2	23	0.38	0.12	0.115	0.044	0.087	111	1.02	0.80	0.557	0.567	0.421
B	2	1	2	0.57	0.04	0.02	0.011	0.015	57	0.78	0.25	0.567	0.443	0.432
C	1	5	40	0.42	0.16	0.08	0.034	0.067	255	1.09	0.72	0.508	0.551	0.425
C	2	5	5	0.41	0.15	0.01	0.004	0.009	242	0.98	0.40	0.486	0.476	0.431
D	1	5	27	0.45	0.22	0.054	0.024	0.041	265	0.84	0.43	0.527	0.444	0.405
D	3	2	9	0.44	0.15	0.045	0.020	0.038	96	0.93	0.51	0.479	0.443	0.403
E	1	4	51	0.40	0.10	0.128	0.051	0.131	76	0.57	0.20	0.190	0.109	0.195
E	2	3	18	0.50	0.11	0.059	0.03	0.097	41	0.51	0.12	0.135	0.069	0.222
F	1	3	34	0.35	0.07	0.113	0.039	0.105	59	0.46	0.13	0.197	0.090	0.181
F	3	1	4	0.34	0.05	0.04	0.013	0.053	27	0.54	0.25	0.267	0.145	0.355

Conf.	Subj.	No. runs avg.	Instrument 6, IVSI						All Instruments		
			N_6	$\bar{T}_{d6}$	σ_{T6}	$\bar{f}_{s6}$	η_6	ν_6	N_M	$\sum T_i$	$\bar{f}_s$
B	1	2	10	0.40	0.14	0.05	0.020	0.038	264	200	1.32
B	2	1	1	0.55	0	0.01	0.005	0.008	132	101	1.31
C	1	5	16	0.38	0.07	0.032	0.012	0.027	600	502	1.19
C	2	5	2	0.47	0.23	0.004	0.002	0.004	561	497	1.13
D	1	5	5	0.40	0.18	0.010	0.004	0.008	654	503	1.30
D	3	2	43	0.45	0.14	0.214	0.095	0.181	238	200	1.19
E	1	4	16	0.44	0.11	0.04	0.018	0.041	390	400	0.976
E	2	3	14	0.49	0.10	0.046	0.023	0.076	185	305	0.607
F	1	3	9	0.35	0.12	0.033	0.012	0.031	325	300	1.08
F	3	1	1	0.49	0	0.01	0.005	0.013	76	101	0.752

change significantly‡ for successive thirds of runs. The dwell time on Instrument 2 in the last one-third of Run 26-09 is significantly smaller than during the first two-thirds because the first two parts each have one very long dwell (i.e., 2.5 sec). If these long dwells are deleted there is no longer a significant difference. The tests for significance were not performed on the dwell fractions, but these data do not show any consistent trends between runs and their variability is probably not significant. Thus these stationarity tests show no important range-varying effects and the EPR can be considered statistically stationary within a run.

Look and Scan Rates

Look rates involve the number of looks/sec on a given instrument, while scan rates involve the entire panel. Analyses of the results in Table 3 show the following. The attitude or attitude/director instrument (No. 2) look rates are generally the same over all pilots and configurations. The HSI/GSD instrument (No. 5) look rates are significantly lower for director than manual ILS runs. The peripheral instrument look rates are scattered and show no strong trends. The all-instrument scan rates are significantly greater for the manual ILS runs than for the director runs. These results correlate with the dwell time and workload results discussed below.

‡ All tests of significance were performed at the 95% confidence level.

Peripheral Instrument Dwell Times

The dwell time is the average length of one instrument fixation. The peripheral instrument results in Table 3 show that:

1) Mean dwell times on the altimeter instruments (No. 3) and IVSI (No. 6) are homogeneous over all pilots and configurations, and are not significantly different from one another. The mean is 0.42 sec.

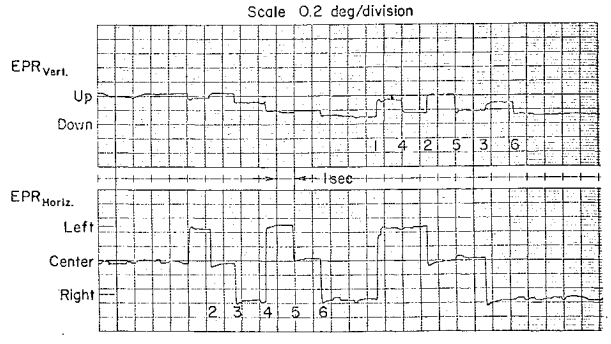

Fig. 7 Illustrative EPR data sample.

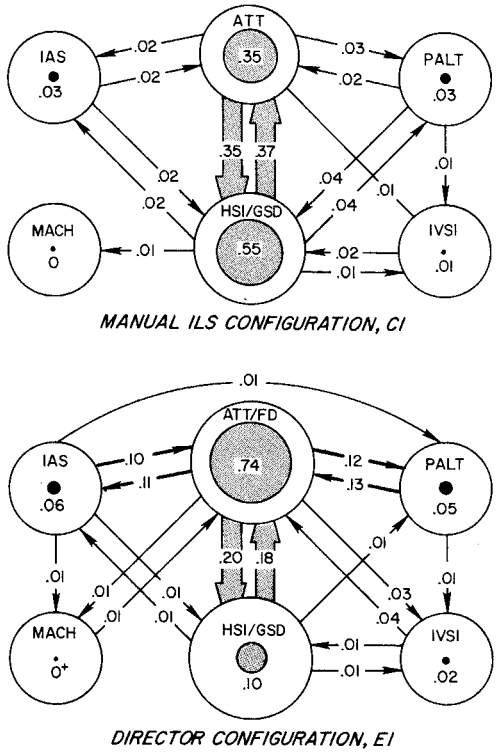

Fig. 8 Typical transition link vectors and dwell fractions.

2) The mean dwell times on the airspeed instrument (No. 1) are homogeneous over all pilots and configurations, and their average (0.64 sec) is significantly greater than for the other peripheral instruments (3 and 6).

Some of the manual ILS data were quantized into 0.05 sec intervals to determine if there was any tendency for discretization in the dwell times (bunched at discrete durations). This did not occur.

Primary Instrument Dwell Times

The dwell time results on the attitude gyro (No. 2) and the HSI/GSD (No. 5) for the various pilots and configurations show that:

1) Mean dwell times on the attitude and HSI/GSD instruments for configuration B are often different from C and D, indicating that the additional lateral axes of control have an effect with some pilots. Note that bank angle is on 2 and localizer deviation and heading are on 5.

2) Differences between fixed and varying range had no effect on the attitude instrument dwell times for either the manual ILS or director configurations. Intrapilot data on similar configurations can be lumped.

3) Fixed vs varying range had a significant effect on the HSI/GSD instrument dwell times for both manual ILS and director configurations. In each case the varying range version had a shorter mean dwell time.

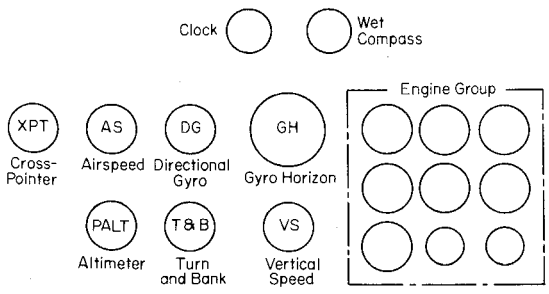

Fig. 9 Standard instrument arrangement used by Fitts et al.,[4,5] and Senders et al.[11]

Table 4 Scanning statistics for run segments

Instrument	Time Interval (sec)	$D1$ (Run 26-05) $\overline{T}_d$	η	$D1$ (Run 26-09) $\overline{T}_d$	η	$F1$ (Run 26-07) $\overline{T}_d$	η
1) IAS							
	0–33	0.67	0.080	0.61	0.056	0.47	0.116
	33–67	0.56	0.050	0.66	0.079	0.65	0.110
	67–100	0.54	0.082	0.50	0.044	0.54	0.102
2) ATT/FD							
	0–33	0.78	0.468	1.02	0.557	1.38	0.716
	33–67	0.84	0.529	0.84	0.477	1.64	0.735
	67–100	0.71	0.500	0.66	0.440	1.25	0.709
3) PALT							
	0–33	0.53	0.031	0.47	0.014	0.40	0.048
	33–67	0.24	0.007	0.44	0.026	0.36	0.040
	67–100	0.50	0.046	0.39	0.034	0.33	0.063
5) HSI/GSD							
	0–33	0.75	0.379	0.68	0.332	0.46	0.099
	33–67	0.69	0.395	0.83	0.395	0.44	0.086
	67–100	0.68	0.354	0.85	0.486	0.43	0.109
6) IVSI							
	0–33	0.32	0.010	0.32	0.010	0.20	0.006
	33–67	0.61	0.018	0.26	0.023	0.40	0.011
	67–100	0	0	0.55	0.016	0.37	0.012

4) The mean dwell times on attitude instrument with the manual ILS configurations are less than with the director at a very high level of significance. The dwell time variances are also much less.

5) The dwell times on the HSI/GSD instrument show the opposite trend. The manual ILS means are greater than the director means at a high level of significance, as are the dwell time variances. These results are consistent because attitude and localizer/glide slope are primary and share 80–90% of the scanning workload.

6) Interpilot differences in mean dwell time on the primary instruments often occurred. These were most pronounced on the attitude instrument with the manual ILS configuration, and did not occur at all on HSI/GSD instrument with the director operating.

Fractional Scanning Workload

The dwell fraction, η_i, also called the fractional scanning workload, is the fraction of time during a run that the pilot is looking at that instrument. Average values for each instrument with each subject/configuration are given in Table 3. Tests of significance were not made, but certain trends are apparent. That is, the dwell fraction on peripheral instruments varies from run to run, but there are no clear differences between pilots or configurations. The dwell fraction on peripheral instruments is much less than that on the primary instruments (by definition). The dwell fractions on the attitude and HSI/GSD instruments are about equal with the manual ILS configurations. The dwell fraction on the attitude instrument is much larger with the director configurations than with the manual ILS ones. The dwell fraction on the HSI/GSD instrument goes way down when the director is in use, and it becomes effectively a peripheral instrument. These differences in scanning workload are due mainly to differences in dwell time, and to some extent changes in scan rate, as shown in Table 3. For example, the unusually low $E2$ scan rate combines with the

Table 5 Comparison of average performance measures for manual versus flight director runs

Performance Measure	Configuration: Manual ILS (C and D)	Configuration: Director (E and F)
σ_{GS_e}	0.072°	0.052°
σ_{θ_c}	2.60°	1.72°
σ_{δ_e}	1.64°	1.9, Pilot 1 3.0, Pilot 2

Table 6 Comparison of dwell fractions with past data

Instrument	STI[a]	Dwell Fraction: Senders[b] (Ref. 11)	Milton[c] (Ref. 4)	Milton[c] (Ref. 6)
Attitude	0.438	0.282	0.15	0.11
HSI/GSD	0.472	0.445	0.655	0.650
PALT	0.018	0.070	0.02	0.02
AS	0.020	0.073	0.10	0.07
IVSI	0.035	0.128	0.05	0.05

[a] Average of three pilots (configurations *C* and *D*).
[b] Average of two pilots (Phase III).
[c] Average of 40 pilots (instrument low approaches).

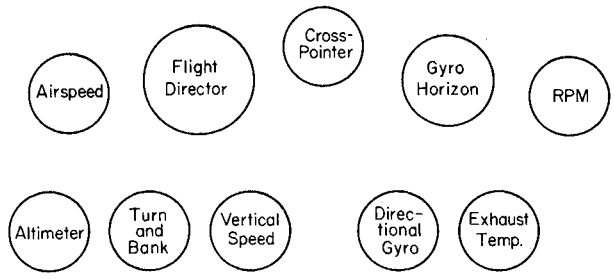

Fig. 10 Panel arrangement used by Milton et al.,[8] for director approaches.

unusually long mean dwell time on the attitude instrument to give the highest observed mean scanning workload.

Transition Links

The one-way link value is the fraction of all fixation transitions that go from one instrument to another. If the pilot is stationary over a run, one-way link values are also indicative of dominant scan patterns. Typical link vectors for Pilot 1 in the manual ILS and director tasks are compared in Fig. 8. The width of the link vector represents its magnitude, and the diameters of the shaded instrument centroids represent the dwell fraction. The sum of the dwell fractions is less than one due to blinks. The data show no dominant circulation of scanning, and the one-way link values (e.g., 2 to 5 and 5 to 2) are approximately equal. The director task has a more evenly distributed percentage of scans to secondary instruments, although a high percent of time was spent on the attitude/flight director indicator. There were very few (<1%) link transitions across instruments, indicating the primary instruments were centrally located.

The big difference between the manual ILS and director configurations is related to the difference in scanning workload. The manual ILS results have dominant links from attitude to HSI/GSD and back. The director links appear more scattered, because these central links are smaller.

Performance Measures

Detailed measures of pilot response and performance were made. Table 5 summarizes the root mean square values of pitch attitude error, glide slope deviation error, and elevator response for the manual ILS and director configurations for Pilots 1 and 2. Interpilot differences were not significant, except for rms elevator with the director, so the data have been lumped as shown. The director runs had significantly lower glide slope deviation and pitch attitude error than the manual ILS runs, with corresponding increased elevator activity. There were no significant differences of the performance measures between the fixed (*C* and *E*) and varying (*D* and *F*) range cases, or between the split axis (*B*) and other (*C* and *D*) manual ILS configurations.

The change in performance with display layout and task is associated with the change in pilot scanning properties described above. For example, the scanning statistics on Instrument 2 show that the look rates are higher and the dwell fractions are larger with the flight director configurations. The relation is not a simple one, however, and its description is a central feature of the theory of manual control displays which is still under development.

Table 7 Comparison of mean dwell times with past data

Instrument	Mean Dwell Time (Sec): STI[a]	Milton (Ref. 6)
Attitude	0.85	0.37
HSI/GSD	0.96	XPT 0.76
		DG 0.54
PALT	0.43	0.38
AS	0.70	0.49
IVSI	0.43	0.39

[a] Weighted average of three pilots (configurations *C* and *D*).

Comparisons with Other Eye Scanning Data

The eye scanning data are generally consistent with the results of prior research, where meaningful comparisons can be made. The largest and most thorough data on pilot eye movements were collected during the early 1950's by Fitts, Milton, Jones, McIntosh, and Cole in a C-45 aircraft using in-flight eye camera films. Similar, more recent, measurements have been made by Senders, Carbonell, and Ward in Ref. 11, utilizing electro-oculograms (EOG) of three subjects in a fixed base fighter simulator. Their panel arrangement was identical to the standard instrument arrangement used by Fitts, et al.,[4,5] and shown in Fig. 9. An "experimental" panel used by Milton, et al.,[6,7] more nearly resembles the panel arrangement used in this program.

The last report of the Air Force series[8] was concerned with director (actually zero reader) approaches. Measurements were made of ten pilots who each flew one approach from the rear seat of a T-33 aircraft. The director indicator was a separate instrument, as shown in Fig. 10.

Manual ILS Data

Table 6 compares dwell fractions from Milton, et al.,[4,6] and Senders, et al.,[11] with the manual ILS data from the DC-8 simulation. The individual dwell fractions of the directional gyro display and the cross-pointer display for the past data were summed to compare with the dwell fractions for the integrated HSI/GSD display. The comparison of available mean dwell times is presented in Table 7. The reduced attention to attitude is probably due to different pilot techniques. For example, the gyro horizon was just replacing the "needle-ball-airspeed" technique during the period of Milton's studies. The current technique supported by nearly all pilots rests primarily on attitude control and there-

Table 8 Comparison of director eye traffic with past data

Instrument	Dwell fraction: STI	Milton (Ref. 8)	Mean dwell time (sec): STI	Milton (Ref. 8)	Scan rate (Looks/sec): STI	Milton (Ref. 8)
[Flight director]	0.77	0.64	1.94	1.29	0.40	0.50
Attitude		0.13		0.48		0.27
[Localizer/glide slope]	0.095	0	0.52	0.25	0.18	0.022
Heading		0.01		0.50		0.02
Airspeed	0.055	0.09	0.55	0.52	0.11	0.168
Vertical Speed	0.02	0.02	0.44	0.45	0.04	0.049
Altimeter	0.04	0.01	0.40	0.42	0.10	0.037
Misc.	0.02	0.10	...	...	0.06	0.46

Table 9 Comparison of averaged two-way link values with past data with director displays

Instrument Links	STI	Milton (Ref. 8)
FD-ATT	Integrated	0.38
FD-AS	0.24	0.24
FD-PALT	0.21	0.04
FD-VS	0.07	0.05
FD-RPM	0	0.06
ATT-RPM	0	0.03
FD-T&B	0	0.03
FD-HSI/GSD	0.41	<0.02

fore has a higher fractional workload and associated dwell time. The peripheral instruments (i.e., PALT, IVSI) are comparable and do show similar workloads and dwell times.

A comparison of the link values between the manual ILS configurations (*C* and *D*) and the experimental panel results of Milton, et al.,[6] may not be meaningful since the number of instruments differed. However, the primary link in the Milton data was the XPT-DG, which is the currently integrated HSI/GSD display. His second largest link, XPT-GH, when combined with the XPT/DG approaches the current HSI/GSD-ATT link value.

Tables 5, 6, and 7 serve to compare rather than evaluate the data. There are many differing factors in the three sets of data which would influence the results. The theory[1] indicates that scanning rates and workload should be strongly influenced by the vehicle dynamic properties. Additional factors noted by Fitts, et al., as having a significant effect on the dwell time and fraction were interpilot differences, day versus night operation, and manual ILS versus ground controlled approaches (GCA).

Director Data

The director data of Ref. 8 are shown in Table 8 with those obtained from the DC-8 simulation (configurations *E* and *F* combined). The dwell fractions (fractional scanning workload) can be added and as such compare very closely with the current attitude/director result. Mean dwell times, a parameter less dependent on vehicle properties, exhibits the same trends between instruments and may have an additive property for integrated displays. The total scan rate in the Ref. 8 study as 92/min or 1.53/sec. This does not compare well to the 0.89/sec in the DC-8 study, and it reflects the difference in aircraft dynamics and pilot technique. The scan rates show that the director is dominant.

The director link values recorded in Ref. 8 support the finding that the one-way links between pairs of instruments are approximately equal, and that the director is the center of attention. Table 9 presents the link values between pairs of instruments, disregarding the values less than 2%.

Summary

Although most of the Milton et al., and Senders et al., data were taken with a panel which differs somewhat from the current T layout, their results can be compared with the new nondirector data. The new data show a larger dwell fraction on the gyro horizon than past data. This may be attributed to differences in panel arrangement and to the evolution of a pilot technique using attitude control. The Milton zero reader dwell fraction data[8] agree well with the present (director configuration) data for most instruments. The exception is that the new data show a larger dwell fraction on HSI/GSD than does the sum of his crosspointer and DG data. The respective dwell times are comparable.

Conclusion

Apparatus is now available which allows the measurement and rapid reduction of eye point-of-regard data for realistic vehicle control tasks. The body of data reported herein are consistent with past data and provide new insight into pilot scanning behavior for instrument approaches. When combined with concurrently measured pilot response data, they will serve to validate and extend the theory of manual control displays.

References

[1] McRuer, D., Jex, H. R., Clement, W. F., and Graham, D., "Development of a Systems Analysis Theory of Manual Control Displays," TR 163-1, Oct. 1967, Systems Technology Inc., Hawthorne, Calif.

[2] Allen, R. W., Clement, W. F., and Jex, H. E., "Research on Display Scanning, Sampling, and Reconstruction Using Separate Main and Secondary Tracking Tasks," CR-1569, July 1969, NASA.

[3] Weir, D. H. and Klein, R. H., "The Measurement and Analysis of Pilot Scanning and Control Behavior during Simulated Instrument Approaches," CR-1535, June 1970, NASA.

[4] Milton, J. L., Jones, R. E., and Fitts, P. M., "Eye Fixations of Aircraft Pilots: Frequency, Duration, and Sequence of Fixations when Flying the USAF Instrument Low Approach Systems (ILAS)," USAF TR 5839, Oct. 1949,

[5] Fitts, P. M., Jones, R. E., and Milton, J. L., "Eye Fixations of Aircraft Pilots: Frequency, Duration, and Sequence of Fixations when Flying Air Force Ground Controlled Approach System (GCA)," AF TR 5967, Feb. 1950,

[6] Milton, J. L., McIntosh, B. B., and Cole, E. L., "Eye Fixations of Aircraft Pilots: Fixations during Day and Night ILAS Approaches using an Experimental Instrument Panel Arrangement," USAF TR 6570, Oct. 1951,

[7] Milton, J. L., McIntosh, B. B., and Cole, E. L., "Eye Fixations on Aircraft Pilots: Fixations during Day and Night GCA Approaches using an Experimental Instrument Panel Arrangement," USAF TR 6709, Feb. 1952,

[8] Milton, J. L. and Wolfe, F. J., "Eye Fixations of Aircraft Pilots: Fixations during Zero Reader Approaches in a Jet Aircraft," WADC TR 52-17, Feb. 1952,

[9] Watts, A. F. A. and Wiltshire, H. C., "Investigation of Eye Movements of an Aircraft Pilot under Blind Approach Conditions," College Note 26, May 1955, The College of Aeronautics, Cranfield, England.

[10] Lennox, D., "Airline Pilot's Eye Movements during Takeoff and Landing in Visual Meteorological Conditions," Human Engineering Note 15, Aug. 1963, Aeronautical Research Labs, Melbourne, Australia.

[11] Senders, J. W., Carbonell, J. R., and Ward, J. L., "Human Visual Sampling Processes: A Simulation Validation Study," CR-1258, Jan. 1969, NASA.

[12] Stapleford, R. L., McRuer, D. T., and Magdaleno, R. E., "Pilot Describing Function Measurements in a Multiloop Task," NASA SP-128, 1966, pp. 181–204.

[13] Stapleford, R. L., Craig, S. J., and Tennant, J. A., "Measurement of Pilot Describing Functions in Single-Controller Multiloop Task," CR-1238, Jan. 1969, NASA.